Motional sideband excitation using rotating electric fields

C. A. Isaac*
Department of Physics, College of Science, Swansea University, Singleton Park, Swansea SA2 8PP, United Kingdom
(Received 26 February 2013; published 15 April 2013)

A form of motional sideband excitation is described in which a rotating dipole electric field is applied asymmetrically onto a Penning-type trap in the presence of a mechanism for cooling the axial motion of the trapped particles. In contrast to the traditional motional sideband excitation, which uses an oscillating electric field, the rotating field results in only one active sideband in each sense of rotation and so avoids accidental excitation of the other sideband making it applicable to Penning-type traps with a large degree of anharmonicity. Expressions are derived for the magnetron radius expansion and compression rates attainable, and approximations are made for the case of strong and weak drives. A comparison is made with data, taken using a two-stage positron accumulator presented by Isaac *et al.* [C. A. Isaac, C. J. Baker, T. Mortensen, D. P. van der Werf, and M. Charlton, Phys. Rev. Lett. **107**, 033201 (2011)], showing good agreement between the model and experiment.

DOI: 10.1103/PhysRevA.87.043415 PACS number(s): 37.10.De, 37.10.Ty, 52.27.Jt

I. INTRODUCTION

Penning-type traps are cylindrically symmetric instruments used for the confinement and study of ions (the term ion is used here to refer to any charged particle, including subatomic particles). A uniform magnetic field, parallel to the trap axis, provides radial confinement while an electric potential minimum, often produced by either a set of hyperbolic electrodes or a series of cylindrical electrodes, is used for axial confinement. Carefully designed Penning traps are capable of exceptionally long confinement times, making them ideal for precision measurements with excellent statistics (see, e.g., [1,2]). In addition to this, Penning-type traps are used for the accumulation and storage of rare and exotic species such as antiparticles and highly charged ions (e.g., [3–5]).

The most harmonic, and hence ideal, region of a Penning-type trap is near the center and so for precision measurements, or simply to produce dense clouds in a Penning trap, limiting motion to near the axis of the trap is desirable. Such axialization results in a reduction in the kinetic energy of the trapped particles and hence the particles are cooled. Cooling is used in this sense only to mean a reduction in kinetic energy and does not imply that when more than one particle is trapped that they are in thermal equilibrium nor that they have a well-defined temperature.

When a sufficiently dense and cold cloud of ions is held in a Penning trap, their mutual interactions cannot be neglected and the ensemble must be treated as a non-neutral plasma. It has been found that the radial extent of such a plasma may be controlled by the application of a rotating electric field, often referred to as the rotating wall technique. This was first demonstrated for ions [6], then electrons [7], and subsequently positrons [8]. Provided a large enough drive amplitude is used, it has been found that the final density of the plasma is dependent on the rotating wall frequency [9,10]; this is the so-called strong-drive regime. The undesirable heating caused by the rotating electric field may be counteracted by collisions with a suitable buffer gas or, in the case of light particles in a strong magnetic field, by the emission of cyclotron radiation.

In the single-particle regime the trapped ions are considered noninteracting, and thus the compression of a cloud of such particles may be described by the transport of the individual ions towards the trap axis; so-called axialization. The method of sideband excitation, first suggested by Wineland and Dehmelt [11,12], uses an inhomogeneous oscillating electric field at specific frequencies to axialize ions in a Penning trap. This technique has been used for a number of measurements [13–15] with various cooling mechanisms employed, including compression of a cloud of antiprotons using a non-neutral buffer gas of electrons [16].

Further to the work of Cassidy *et al.* [17], Greaves and Moxom have shown that it is possible to compress a cloud of positrons in the single-particle regime by the application of an axially asymmetric rotating electric field [18]. They attributed this to the phenomenon of asymmetric bounce resonance, though this effect has only been investigated theoretically and experimentally in the plasma limit [19–22].

Isaac *et al.* [23] have recently demonstrated that a rotating electric field can be used to compress a cloud of positrons and they derived compression rates at various amplitudes and frequencies of the applied field. They also outlined a theoretical model which showed good agreement with the experimental data, though aspects of their trap and technique resulted in effects beyond the scope of the model treatment.

This paper provides a more complete treatment of the effect of an axially asymmetric rotating dipole electric field on the motion of a charged particle within a Penning trap with the presence of a cooling term described by a Stokes viscous drag than is presented in [23], along with some additional results. To begin, a review is presented of the theory of the ideal Penning trap followed by the case of an oscillating dipole electric field as described in [13]. Comparisons are drawn between the cases of the oscillating and rotating dipoles showing that the axializing effects are of a similar origin, but with the latter being applicable to a wider range of traps as it results in only one active sideband in each direction of rotation. Finally, the predictions of this model are compared with experimental data.

*c.a.isaac@swansea.ac.uk

II. THE IDEAL PENNING TRAP

The ideal Penning trap electric potential is a quadratic minimum along the trap axis and, subject to Laplace's equation, may be written in cylindrical coordinates (r,θ,z) as

$$\phi = \frac{\omega_z^2 m}{2q}\left(z^2 - \frac{r^2}{2}\right), \tag{1}$$

where ω_z is the bounce frequency of the trapped particle of mass m and charge q. Superimposed on this is a magnetic field conventionally parallel to the trap axis, $\mathbf{B} = B_0\hat{z}$, and so the Lorentz force gives the axial equation of motion for a charged particle as a harmonic oscillator,

$$\frac{d^2 z}{dt^2} + \omega_z^2 z = 0, \tag{2}$$

and the radial equation of motion as

$$\frac{d^2\mathbf{r}}{dt^2} + \Omega\hat{z}\times\frac{d\mathbf{r}}{dt} - \frac{\omega_z^2}{2}\mathbf{r} = 0, \tag{3}$$

where $\Omega = qB_0/m$ is the cyclotron frequency as exhibited by a charged particle in a uniform magnetic field. A large number of texts give a thorough treatment of the Penning trap (see, e.g., [24]). Using a set of coordinates[1] defined by

$$\mathbf{V}^{\pm} = \frac{d\mathbf{r}}{dt} + \omega_{\mp}\hat{z}\times\mathbf{r}, \tag{4}$$

where

$$\omega_{\pm} = \frac{1}{2}\left(\Omega \pm \sqrt{\Omega^2 - 2\omega_z^2}\right), \tag{5}$$

allows the radial equation of motion to be written as

$$\frac{d}{dt}\mathbf{V}^{\pm} = -\omega_{\pm}\hat{z}\times\mathbf{V}^{\pm}, \tag{6}$$

which has the solutions

$$\mathbf{V}^{\pm} = A^{\pm}\begin{pmatrix}\sin(\omega_{\pm}t - \phi_{\pm})\\ \cos(\omega_{\pm}t - \phi_{\pm})\end{pmatrix}. \tag{7}$$

$A^{\pm}$ and $\phi_{\pm}$ are amplitudes and phases which are dependent on the initial conditions. Taking the difference $\mathbf{V}^+ - \mathbf{V}^-$ and crossing with $\hat{z}$ returns the radial coordinate:

$$\mathbf{r} = \begin{pmatrix}x\\ y\end{pmatrix} = \frac{\hat{z}\times(\mathbf{V}^+ - \mathbf{V}^-)}{\omega_+ - \omega_-}. \tag{8}$$

Thus the radial motion of the particle is given by a superposition of two circular motions: one with an angular frequency ω_+ termed the modified cyclotron motion, and one with an angular frequency of ω_- called the magnetron motion. In a Penning trap the frequencies typically have the hierarchy $\omega_+ \gg \omega_z \gg \omega_-$.

The energy stored in the cyclotron motion is almost purely kinetic, while in the axial motion it oscillates between kinetic and potential. In contrast to these, the energy stored in the magnetron motion is almost purely potential. The magnetron motion of the ion may be thought of as rolling around the top of a potential hill and so removing energy will result in the orbit expanding.

Damping of the ion motion may be modeled by a Stokes viscous drag force; $\mathbf{F} = -\kappa\mathbf{v}$, where κ is a drag coefficient. Such damping is achievable by the use of a background buffer gas (neglecting the associated Langevin force) where κ is related to the mobility of the trapped ion in the gas. The viscous drag force modifies the axial motion, given by Eq. (2), to that of a damped harmonic oscillator with a damping rate κ. The motion in the radial plane is modified to [16]

$$\mathbf{V}^{\pm} = A^{\pm}e^{\alpha_{\pm}t}\begin{pmatrix}\sin(\omega_{\pm}t - \phi_{\pm})\\ \cos(\omega_{\pm}t - \phi_{\pm})\end{pmatrix}, \tag{9}$$

where

$$\alpha_{\pm} \approx \mp\kappa\frac{\omega_{\pm}}{\omega_+ - \omega_-}. \tag{10}$$

Given the typical frequency hierarchy in a Penning trap, both the axial and modified cyclotron motions are damped at a rate $\approx\kappa$, however, the magnetron motion will slowly expand at a rate $\approx\kappa(\omega_-/\omega_+)$ until the particle is lost from the trap. This expansion can be counteracted by coupling the three different motions by the addition of typically rf electric fields which are applied either to segments of the existing electrodes, or by the inclusion of additional electrodes to the Penning-type trap assembly.

III. EXCITATION BY AN OSCILLATING DIPOLE

The normally decoupled radial and axial motions may be coupled by the application of an inhomogeneous oscillating electric field. Given that $\mathbf{V}^{\pm}$ resonates at frequencies $\omega_{\pm}$ it may be seen that near the bounce frequency ω_z only the magnetron motion $\mathbf{V}^-$ will contribute significantly. Thus for the remainder of this paper the cyclotron motion is neglected ($\mathbf{V}^+ = 0$) and we set $\mathbf{V}^- = (V_x, V_y)$. The time scale for the expansion of the magnetron motion is also considered large enough such that only the damping in the axial direction is of significance.

This cooling model approximation makes the derivation which follows applicable when resistive cooling is used. Here the energy of the trapped particle is dissipated in a resistor connected between the trap electrodes producing a cooling term which is proportional to the ion velocity (see [13] for a full discussion).

The electric potential of an axially asymmetric oscillating dipole with frequency ω_r may be written in Cartesian coordinates as

$$\phi_{\text{osc}} = a\frac{m}{q}zx\,\cos(\omega_r t), \tag{11}$$

where a is the oscillating field amplitude. With the addition of a Stokes viscous drag term to simulate a cooling mechanism along the axis of the trap, the superposition of the oscillating potential onto the ideal Penning trap potential given in Eq. (1) modifies the equations of motion as

$$\left(\frac{d^2}{dt^2} + \kappa\frac{d}{dt} + \omega_z^2\right)z = -ax\,\cos(\omega_r t), \tag{12}$$

$$\frac{dV_x}{dt} = \omega_- V_y - az\,\cos(\omega_r t), \tag{13}$$

[1] In [13] a negative sign is used for the second term in Eq. (4) such that the magnetic field lies antiparallel to the trap axis.

and

$$\frac{dV_y}{dt} = -\omega_- V_x. \tag{14}$$

The time derivative of Eq. (14) substituted into Eq. (13) gives

$$\left(\frac{d^2}{dt^2} + \omega_-^2\right) V_y = a\omega_- z \cos(\omega_r t). \tag{15}$$

Also, using Eqs. (8) and (12) yields

$$\left(\frac{d^2}{dt^2} + \kappa\frac{d}{dt} + \omega_z^2\right) z = -\frac{a}{\omega_+ - \omega_-} V_y \cos(\omega_r t), \tag{16}$$

which closes the equations of motion.

An insight into the mechanism responsible for the compression or expansion of the magnetron motion may be obtained by inserting the short-term magnetron behavior (neglecting the phase and amplitude) $V_y \sim \cos(\omega_- t)$ into Eq. (16):

$$\left(\frac{d^2}{dt^2} + \kappa\frac{d}{dt} + \omega_z^2\right) z \sim -\frac{a}{\omega_+ - \omega_-}\{\cos[(\omega_r - \omega_-)t] + \cos[(\omega_r + \omega_-)t]\}. \tag{17}$$

This is a harmonic oscillator with two driving frequencies. Let one of these frequencies be resonant with the oscillator, which is the case when $\omega_r = \omega_z \pm \omega_-$, giving

$$\left(\frac{d^2}{dt^2} + \kappa\frac{d}{dt} + \omega_z^2\right) z \sim -\{\cos(\omega_z t) + \cos[(\omega_z \pm 2\omega_-)t]\}. \tag{18}$$

Under a narrow resonance approximation ($\kappa \ll \omega_-$) the second term will have a negligible effect, such that the resonantly driven axial motion behaves as

$$z \sim -\cos\left(\omega_z t - \frac{\pi}{2}\right) \equiv -\sin(\omega_z t). \tag{19}$$

Inserting this solution into Eq. (15) gives

$$\left(\frac{d^2}{dt^2} + \omega_-^2\right) V_y \sim \omega_-\{\pm\sin(\omega_- t) - \sin[(2\omega_z \pm \omega_-)t]\}. \tag{20}$$

Given the typical frequency hierarchy, the second term is highly nonresonant with the oscillator and so neglecting it yields

$$\left(\frac{d^2}{dt^2} + \omega_-^2\right) V_y \sim \mp[-\omega_- \sin(\omega_- t)] \equiv \mp\frac{dV_y}{dt}, \tag{21}$$

which behaves as a damping force in the case of the upper sign and an antidamping force in the case of the lower sign.

To derive an equation governing the magnetron radius expansion and compression rates, the drive frequency must be allowed to deviate away from resonance by a small amount, ϵ, such that $\omega_r = \omega_z \pm \omega_- + \epsilon$, and a solution is sought in which the magnetron behavior is $V_y = Ae^{-i\omega t}$ with $\omega \approx \omega_-$ and A a constant. Using this behavior in Eq. (16) gives

$$\begin{aligned}\left(\frac{d^2}{dt^2} + \kappa\frac{d}{dt} + \omega_z^2\right) z &= -\frac{aA}{2(\omega_+ - \omega_-)}\left(e^{i[\pm\omega_z + (\omega_- - \omega)\pm\epsilon]t} + e^{i[\mp\omega_z - (\omega_- + \omega)\mp\epsilon]t}\right) \\ &\approx -\frac{aA}{2(\omega_+ - \omega_-)} e^{i[\pm\omega_z + (\omega_- - \omega)\pm\epsilon]t}\end{aligned} \tag{22}$$

and so, since this is a driven oscillator, the axial motion behaves as

$$z = Be^{i[\pm\omega_z + (\omega_- - \omega)\pm\epsilon]t}, \tag{23}$$

with B another constant. Inserting z back into Eq. (15) gives

$$\begin{aligned}\left(\frac{d^2}{dt^2} + \omega_-^2\right) V_y &= \frac{a\omega_- B}{2}\left(e^{-i\omega t} + e^{i(\pm 2\omega_z + 2\omega_- - \omega \pm 2\epsilon)t}\right) \\ &\approx \frac{a\omega_- B}{2} e^{-i\omega t}\end{aligned} \tag{24}$$

as desired. Thus, the two second-order differential equations have been transformed into an algebraic pair. With some further approximations based on the frequency hierarchy these may be written in matrix form $\mathcal{M}\mathbf{x} = 0$ as

$$\begin{pmatrix} \pm\left((\omega - \omega_-) - \epsilon + i\frac{\kappa}{2}\right) & \frac{a}{4\omega_z(\omega_+ - \omega_-)} \\ \frac{a}{4} & (\omega - \omega_-) \end{pmatrix} \begin{pmatrix} B \\ A \end{pmatrix} = 0, \tag{25}$$

which will only have a solution if the determinant of the matrix $\mathcal{M}$ vanishes. This condition is met when

$$(\omega - \omega_-)^2 + (i\gamma - \epsilon)(\omega - \omega_-) \mp \frac{\delta_{\text{osc}}^2}{4} = 0, \tag{26}$$

where $\gamma = \kappa/2$ and

$$\delta_{\text{osc}}^2 = \left(\frac{a}{2}\right)^2 \frac{1}{\omega_z(\omega_+ - \omega_-)}. \tag{27}$$

Equation (27) governs the magnetron behavior and it will be shown in the next section that an equation of the same form holds for a rotating dipole electric field applied to a particle in a Penning trap. These equations will be solved in Sec. V to derive an analytic expression for the compression and expansion rates.

IV. EXCITATION BY A ROTATING DIPOLE

The electric potential of an axially asymmetric rotating dipole may be written as

$$\phi_r = a\frac{m}{q} z[x\cos(\omega_r t) - y\sin(\omega_r t)]. \tag{28}$$

With the addition of a Stokes viscous drag term, as in the previous section, the superposition of this potential onto the ideal Penning-trap potential modifies the equations of motion as

$$\left(\frac{d^2}{dt^2}+\kappa\frac{d}{dt}+\omega_z^2\right)z=-a\left[x\,\cos(\omega_r t)-y\,\sin(\omega_r t)\right], \tag{29}$$

$$\frac{dV_x}{dt}=\omega_- V_y - az\,\cos(\omega_r t), \tag{30}$$

and

$$\frac{dV_y}{dt}=-\omega_- V_x + az\,\sin(\omega_r t). \tag{31}$$

Substituting the time derivative of Eq. (31) into Eq. (30) gives

$$\left(\frac{d^2}{dt^2}+\omega_-^2\right)V_x=a\left[(\omega_r+\omega_-)\,z\,\sin(\omega_r t)-\dot z\,\cos(\omega_r t)\right]. \tag{32}$$

Similarly the substitution of the time derivative of Eq. (30) in Eq. (31) produces

$$\left(\frac{d^2}{dt^2}+\omega_-^2\right)V_y=a\left[(\omega_r+\omega_-)\,z\,\cos(\omega_r t)+\dot z\,\sin(\omega_r t)\right]. \tag{33}$$

Finally, combining the results given in Eqs. (8) and (29) yields

$$\left(\frac{d^2}{dt^2}+\kappa\frac{d}{dt}+\omega_z^2\right)z = -\frac{a}{\omega_+-\omega_-}\left[V_y\cos(\omega_r t)+V_x\sin(\omega_r t)\right], \tag{34}$$

closing the equations of motion. Again, an insight into the compression and expansion mechanisms may be obtained using the short-term magnetron behavior (neglecting phase and amplitude), $V_y\sim\cos(\omega_- t)$ and $V_x\sim\sin(\omega_- t)$, in Eq. (29):

$$\left(\frac{d^2}{dt^2}+\kappa\frac{d}{dt}+\omega_z^2\right)z\sim-\frac{a}{\omega_+-\omega_-}\cos(\omega_r-\omega_-)\,t. \tag{35}$$

This equation highlights an important difference between the case of the oscillating and rotating dipoles. In contrast to the result given in Eq. (17), the short-term magnetron behavior has resulted in a driving force on the axial motion at only a *single* frequency, thus removing the requirement, in the rotating case, for traps with narrow resonances to prevent overlap of the two sidebands. Examining this term shows that a drive at the lower sideband frequency ($\omega_r=\omega_z-\omega_-$) does not produce a resonant response; the sideband is inactive. A resonant response is, however, obtained at the drive frequencies[2] $\omega_r=\pm\omega_z+\omega_-$ giving a resonant axial response:

$$z\sim-\cos\left(\omega_z t-\frac{\pi}{2}\right)\equiv-\sin(\omega_z t). \tag{36}$$

Inserting this axial behavior into Eq. (32) gives

$$\left(\frac{d^2}{dt^2}+\omega_-^2\right)V_x \sim \mp 2\omega_-\cos(\omega_- t)+2(\omega_z\pm\omega_-)\cos(\pm 2\omega_z+\omega_-)\,t, \tag{37}$$

[2]For the oscillating dipole, a frequency of $\pm\omega_z$ is equivalent irrespective of the sign as the field does not have a sense of rotation.

which, neglecting the nonresonant second term, gives

$$\left(\frac{d^2}{dt^2}+\omega_-\right)V_x\sim\mp\omega_-\cos(\omega_- t)\equiv\mp\frac{dV_x}{dt}. \tag{38}$$

The upper sign corresponds to a damping term, while the lower gives an antidamping force on the magnetron motion. A similar result can be obtained for V_y using the resonant axial behavior in Eq. (33).

Following the analysis used to derive the equation governing the expansion and compression rates in the case of the oscillating dipole, as given in the previous section, we allow the drive frequency to deviate away from the resonant frequencies by a small amount ϵ such that $\omega_r=\pm\omega_z+\omega_-+\epsilon$, and look for a solution in which the magnetron motion is $V_x=iAe^{-i\omega t}$ and $V_y=Ae^{-i\omega t}$ with $\omega\approx\omega_-$. Substituting this behavior into Eq. (34) gives

$$\left(\frac{d^2}{dt^2}+\kappa\frac{d}{dt}+\omega_z^2\right)z=-A\frac{a}{\omega_+-\omega_-}e^{i(\pm\omega_z+\omega_--\omega+\epsilon)t}, \tag{39}$$

and so the axial motion, as a driven oscillator, is given by

$$z=Be^{i(\pm\omega_z+\omega_--\omega+\epsilon)t}. \tag{40}$$

Inserting this result into Eq. (32) gives the desired behavior,

$$\begin{aligned}\left(\frac{d^2}{dt^2}+\omega_-\right)V_y &= B\frac{a}{2}[(\omega_-+\omega)e^{-i\omega t}+(\pm 2\omega_z+3\omega_- \\ &\quad +2\epsilon-\omega)e^{i(\pm 2\omega_z+2\omega_-+2\epsilon-\omega)t}] \\ &\approx B\frac{a}{2}(\omega_-+\omega)\,e^{-i\omega t}.\end{aligned} \tag{41}$$

Again, a similar expression may be obtained for V_x by inserting the axial behavior into Eq. (33). Thus, we have transformed the second-order differential equations into algebraic equations. The algebraic equations relating to Eqs. (32) and (33) are self-consistent and so only one is needed. With some further approximations, analogous to the previous section, the result may be written in matrix form $\mathcal{M}\mathbf{x}=0$ as

$$\begin{pmatrix}\pm\left(\omega-\omega_--\epsilon+i\frac{\kappa}{2}\right) & \dfrac{a}{2\omega_z(\omega_+-\omega_-)}\\ -\dfrac{a}{2} & (\omega_--\omega)\end{pmatrix}\begin{pmatrix}B\\A\end{pmatrix}=0. \tag{42}$$

The determinant of the matrix will vanish when

$$(\omega-\omega_-)^2+(i\gamma-\epsilon)(\omega-\omega_-)\mp\frac{\delta_r^2}{4}=0, \tag{43}$$

where $\gamma=\kappa/2$ and

$$\delta_r^2=a^2\frac{1}{\omega_z(\omega_+-\omega_-)}. \tag{44}$$

This is an identical condition to that given in Eq. (26) for the oscillating dipole electric field, but with $\delta_r=2\delta_{\rm osc}$. In the next section Eqs. (26) and (43) will be solved giving an analytic expression for the expansion and compression rates.

V. COOLING AND HEATING RATES

It has been shown that in the case of the oscillating dipole, applied with $\omega_r=\omega_z\pm\omega_-+\epsilon$, and the rotating dipole, applied with $\omega_r=\pm\omega_z-\omega_-+\epsilon$, the magnetron motion is governed by Eqs. (26) and (43), respectively, both of which are of the form

$$(\omega - \omega_-)^2 + (i\gamma - \epsilon)(\omega - \omega_-) \mp \frac{\delta^2}{4} = 0, \tag{45}$$

the solution of which is given by

$$\omega = \omega_- - \tfrac{1}{2}(-(i\gamma - \epsilon) \pm_s \sqrt{(i\gamma - \epsilon)^2 \pm \delta^2}). \tag{46}$$

The notation $\pm_s$ is used to distinguish between the $\pm$ of the root and the $\pm$ of ω_r. The real part of ω corresponds to an adjusted magnetron frequency and the imaginary part to a magnetron radius compression and expansion rate. The solution of interest gives $\omega \to \omega_-$ in the limit $a \to 0$ and so $\pm_s = -1$. (For a discussion of the other limit, corresponding to an axial excitation, see [13].)

Given this, the compression and expansion rate of the magnetron radius Γ may be written in a dimensionless form as

$$\frac{2\Gamma}{\gamma} = 1 - \sqrt{\frac{2\xi^2}{\sqrt{\xi^4 + 2(\pm\eta^2 + 1)\xi^2 + (\pm\eta^2 - 1)^2} + \xi^2 \pm \eta^2 - 1}}, \tag{47}$$

where $\eta = \delta/\gamma$ is a measure of the drive strength to damping radio and $\xi = \epsilon/\gamma$ is a measure of the detuning to damping ratio; this is shown graphically in Fig. 1. A weak drive limit may be taken in which $\eta \ll 1$ by performing a Taylor expansion of Γ in η giving a Lorentzian line shape as

$$\frac{2\Gamma}{\gamma} = \frac{\eta^2}{2(1 + \xi^2)}. \tag{48}$$

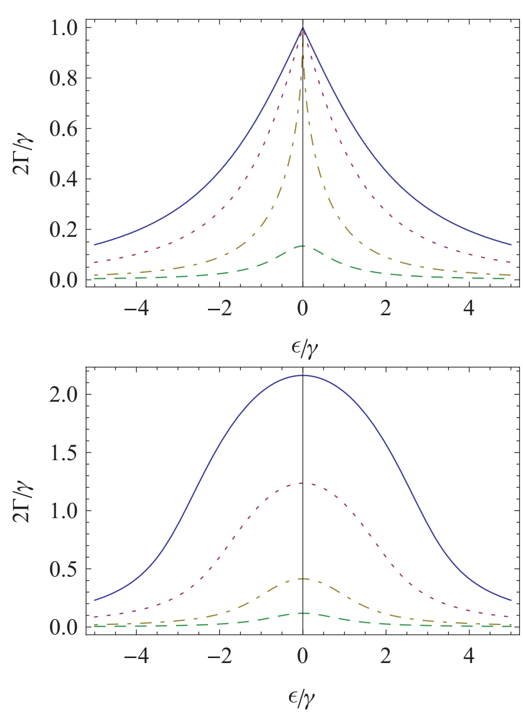

FIG. 1. (Color online) The normalized line shape for the compression rate (top) and for the expansion rate (bottom) of the magnetron orbit as given by Eq. (47), $2\Gamma/\gamma$, as a function of the detuning frequency ϵ, where δ/γ is 3 (navy blue solid), 2 (red dotted), 1 (yellow dot-dashed), and 0.5 (green dashed). γ is the damping strength and δ is given by Eqs. (27) and (44) for the case of the oscillating and rotating dipole electric fields, respectively.

This equation is valid for both the expansion and compression rates of the magnetron radius. The strong drive limit in which $\eta \gg 1$ may be taken for the case of compression as

$$\frac{2\Gamma}{\gamma} = 1 - \sqrt{\frac{\xi^2}{\xi^2 + \eta^2}}. \tag{49}$$

Both these limits are shown graphically in Fig. 2. The limit for the expansion rate of the magnetron motion under a strong drive cannot be taken.

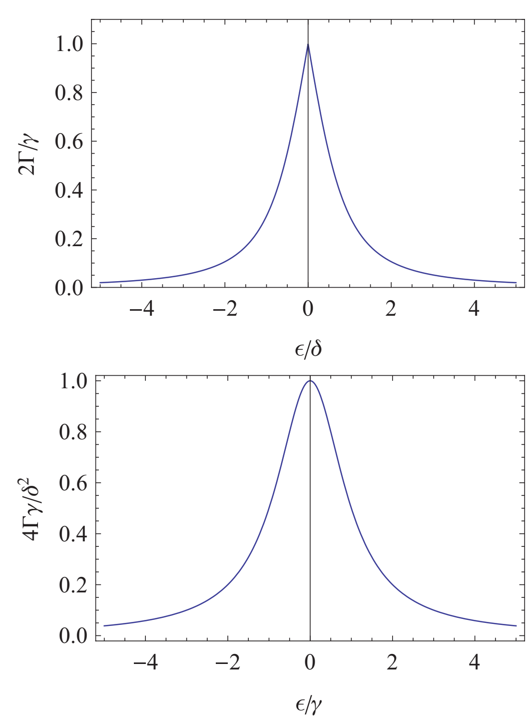

FIG. 2. (Color online) The normalized line shapes for the expansion and compression rates as a function of the detuning frequency ϵ with a strong drive $\delta/\gamma \gg 1$ (upper) and a weak drive $\delta/\gamma \ll 1$ (lower). The weak drive approximation is valid for both compression and expansion, however, the strong drive approximation is only valid in the case of compression.

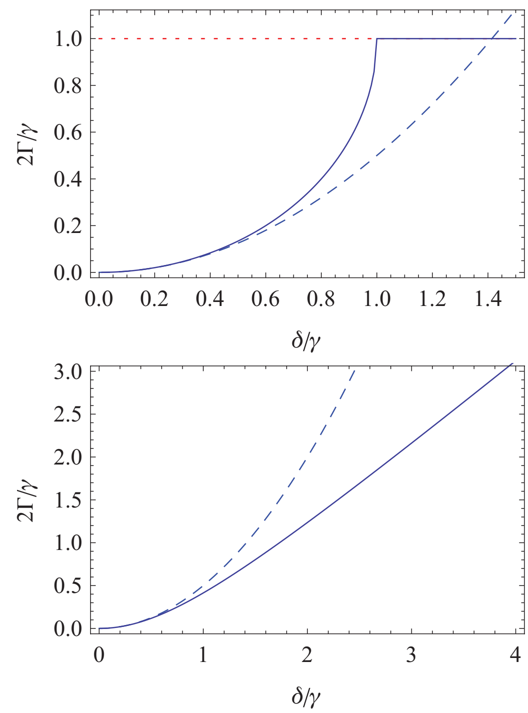

FIG. 3. (Color online) The normalized maximum compression (top) and expansion (bottom) rates $2\Gamma/\gamma$, which are achieved on resonance ($\epsilon = 0$). Shown is the full solution (navy blue solid), the strong drive $\delta/\gamma \gg 1$ (red dotted), and the weak drive $\delta/\gamma \ll 1$ (blue dashed).

An investigation into the maximum compression and expansion rates which is obtained on resonance $\lim_{\epsilon\to 0}(\Gamma)$ shows that for a weak drive both the maximum compression and expansion rates Γ are equal to $\delta^2/(4\gamma)$, while for a strong drive the maximum compression rate is fixed at $\gamma/2$. These are shown graphically in Fig. 3. In a poorly designed Penning trap, given that the two sidebands in the case of the oscillating dipole are only separated by $2\omega_-$, the compression and expansion line profiles may overlap and so expansion will most likely overcome compression resulting in heating of the ion. This is not a problem for the rotating dipole as compression and expansion occur with the electric field rotating in opposite directions, and so accidental heating can be avoided.

VI. COMPARISON WITH EXPERIMENT

A separate paper has been published [23] showing experimental data taken with a two-stage positron accumulator which shows good agreement with this model, although the specifics of the trap complicate the detail. The trap used a series of cylindrical electrodes to produce the electric potential minimum. To one side of the potential minimum one of the electrodes was divided azimuthally into four equal sectors and a sinusoidal voltage applied to each successive sector, in quadrature, producing a rotating, predominantly dipolar, electric field near the center of the trap. Cooling was provided by collisions on SF_6 gas in the trap.

A cloud of positrons was accumulated, compressed, and the radial extent measured. Fitting an exponential to this parameter as a function of compression time allowed a compression rate to be determined for each applied rotating electric field frequency. The results of a series of such measurements are shown in Fig. 4 together with a fit of the form predicted by Eq. (49). As can be seen, the experimentally determined and the predicted line shapes are in good agreement.

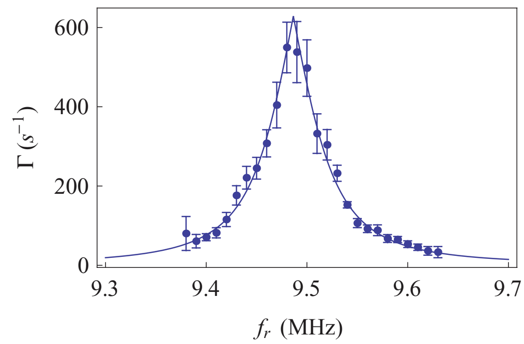

FIG. 4. (Color online) Experimental data from [23] showing the measured compression rate Γ as a function of the applied rotating electric field frequency $f_r = \omega_r/(2\pi)$. The solid line is a fit of the form given by Eq. (49) for the strong drive approximated compression rate.

The effect described in this paper may qualitatively account for the compression observed by Greaves and Moxom [18] and Cassidy *et al.* [17]. Direct comparison of their experimental data with this model cannot be made as they measured the central density of a distribution of particles. Such measurements would seem to represent a convolution of the compression of their cloud with any effects which could cause a change in their trapped particle number, such as heating and axial resonance. In addition to this, the anharmonicities in both of these traps may distort the compression rate line shapes significantly.

VII. SUMMARY

A mechanism has been suggested for the axialization of particles in Penning-type traps by the application of an axially asymmetric rotating dipole electric field in the presence of a suitable cooling mechanism, and appropriate magnetron radius expansion and compression rates have been derived. An important difference between the oscillating and rotating cases has been found: The requirement for very narrow resonances to prevent overlap of the upper and lower sidebands is removed in the latter as only one of the sidebands is active in each direction of rotation and so accidental heating caused by excitation of the wrong sideband can be avoided. This opens the possibility of using this technique for traps with a large degree of anharmonicity, including two-stage positron accumulators [25–27], provided the ion density is kept below the plasma limit.

ACKNOWLEDGMENTS

I am grateful to Professor Mike Charlton and Dr. Dirk van der Werf for numerous helpful discussions and support. I thank the EPSRC for its financial support of the program currently via EP/H026932/1.

[1] R. S. Van Dyck, P. B. Schwinberg, and H. G. Dehmelt, Phys. Rev. Lett. **59**, 26 (1987).
[2] G. Gabrielse, X. Fei, L. A. Orozco, R. L. Tjoelker, J. Haas, H. Kalinowsky, T. A. Trainor, and W. Kells, Phys. Rev. Lett. **65**, 1317 (1990).
[3] T. J. Murphy and C. M. Surko, Phys. Rev. A **46**, 5696 (1992).
[4] G. Gabrielse, X. Fei, K. Helmerson, S. L. Rolston, R. Tjoelker, T. A. Trainor, H. Kalinowsky, J. Haas, and W. Kells, Phys. Rev. Lett. **57**, 2504 (1986).
[5] D. Schneider, D. A. Church, G. Weinberg, J. Steiger, B. Beck, J. McDonald, E. Magee, and D. Knapp, Rev. Sci. Instrum. **65**, 3472 (1994).
[6] X.-P. Huang, F. Anderegg, E. M. Hollmann, C. F. Driscoll, and T. M. O'Neil, Phys. Rev. Lett. **78**, 875 (1997).
[7] F. Anderegg, E. M. Hollmann, and C. F. Driscoll, Phys. Rev. Lett. **81**, 4875 (1998).
[8] R. G. Greaves and C. M. Surko, Phys. Rev. Lett. **85**, 1883 (2000).
[9] J. R. Danielson and C. M. Surko, Phys. Rev. Lett. **94**, 035001 (2005).
[10] J. R. Danielson, C. M. Surko, and T. M. O'Neil, Phys. Rev. Lett. **99**, 135005 (2007).
[11] D. Wineland and H. Dehmelt, Int. J. Mass Spectrom. Ion Phys. **16**, 338 (1975); **19**, 251 (1976).
[12] H. G. Dehmelt, Nature (London) **262**, 777 (1976).
[13] L. S. Brown and G. Gabrielse, Rev. Mod. Phys. **58**, 233 (1986).
[14] H. F. Powell, D. M. Segal, and R. C. Thompson, Phys. Rev. Lett. **89**, 093003 (2002).
[15] G. Savard, S. Becker, G. Bollen, H. J. Kluge, R. B. Moore, T. Otto, L. Schweikhard, H. Stolzenberg, and U. Wiess, Phys. Lett. A **158**, 247 (1991).
[16] A. Kellerbauer *et al.* (ATHENA Collaboration), Phys. Rev. A **73**, 062508 (2006).
[17] D. B. Cassidy, S. H. M. Deng, R. G. Greaves, and A. P. Mills, Jr., Rev. Sci. Instrum. **77**, 073106 (2006).
[18] R. G. Greaves and J. M. Moxom, Phys. Plasmas **15**, 072304 (2008).
[19] D. L. Eggleston and T. M. O'Neil, Phys. Plasmas **6**, 2699 (1999).
[20] R. G. Greaves and C. M. Surko, Phys. Plasmas **8**, 1879 (2001).
[21] D. L. Eggleston and B. Carrillo, Phys. Plasmas **9**, 786 (2002).
[22] D. L. Eggleston and B. Carrillo, Phys. Plasmas **10**, 1308 (2003).
[23] C. A. Isaac, C. J. Baker, T. Mortensen, D. P. van der Werf, and M. Charlton, Phys. Rev. Lett. **107**, 033201 (2011).
[24] P. K. Ghosh, *Ion Traps* (Oxford University Press, New York, 1996).
[25] J. Clarke, D. P. van der Werf, B. Griffiths, D. C. S. Beddows, M. Charlton, H. H. Telle, and P. R. Watkeys, Rev. Sci. Instrum. **77**, 063302 (2006).
[26] R. G. Greaves and J. Moxom, *Design and Performance of a Trap-Based Positron Beam Source*, AIP Conf. Proc. No. 692 (AIP, Melville, NY, 2003), p. 140.
[27] J. Clarke, D. P. van der Werf, M. Charlton, D. Beddows, B. Griffiths, and H. H. Telle, *Developments in the Trapping and Accumulation of Slow Positrons using the Buffer Gas Technique*, AIP Conf. Proc. No. 692 (AIP, Melville, NY, 2003), p. 178.